Electrical Power and Energy Systems 150 (2023) 109089

Contents lists available at ScienceDirect

International Journal of Electrical Power and Energy Systems

journal homepage: www.elsevier.com/locate/ijepes

Age-dependent resilience assessment and quantification of distribution systems under extreme weather events

Farshid Dehghani [a], Mohammad Mohammadi [a,*], Mazaher Karimi [b]

[a] Department of Power and Control, School of Electrical and Computer Engineering, Shiraz University, Shiraz ,Iran
[b] School of Technology and Innovations, University of Vaasa, Vaasa, Finland

ARTICLE INFO

Keywords:
Resiliency assessment
Resilience quantification metrics
Power distribution system
Failure probability
Restoration time
Extreme weather events

ABSTRACT

The impact of extreme weather events on power system resilience can be seen in historical electrical disruptions. Due to the increasing intensity and frequency of extreme weather events following global warming and climate change, a greater focus is required to design power systems with high resilience and low cost through assessing and quantifying power system resilience. In this way, we propose a transparent methodology and a set of metrics to quantify the resilience of distribution systems subjected to hurricanes. This methodology includes a probabilistic and detailed approach to modelling the failure probability of overhead lines and the restoration time of damaged lines. Moreover, the fragility analysis of the power system infrastructure is considered age-dependent, and the system's resilience by considering different lifetimes is assessed. The time-dependent resilience assessment constitutes an essential component in risk-informed decision-making for resilience enhancement strategies in the future. Specifically, this paper provides two resilience curve-based metrics: vulnerability rate and restoration rate. The first metric indicates the power system's ability to resist extreme events, and the second indicates its ability to bounce back to normal performance. Simulations are performed on the IEEE 69-bus distribution test system to validate the suggested methodologies. The results indicate the capability of the proposed methodology and metrics to precisely assess and quantify the power system resilience. A significant correlation between the age of power distribution systems and the system's resilience can be seen. These findings can support decision-making concerning system management and plans such as expansion planning and resource allocation.

1. Introduction

1.1. Background and motivation

Extreme weather events, as low-probability and high-impact events, have led to significant social, economic, physical disruptions, and even human casualties worldwide [1]. Power systems as critical infrastructures (CIs) are vulnerable to extreme weather events due to their spread across geographical areas and the increasing intensity of natural hazards. Thus, resiliency assessment is a crucial tool for assessing risks brought by extreme weather events in the power systems and providing prior knowledge for preventing programs. Hence, this study focuses on two main aims, including i) assessment and ii) quantification of resiliency in power systems.

On the one hand, many studies on the resiliency of distribution systems have focused on resilience enhancement [2]. In addition, several papers refer to the resilience assessment of distribution systems. However, few of them focused on the failure probability of overhead lines, restoration time of damaged lines, and the fragility curve of vulnerable components in detail. So, it is necessary to consider a probabilistic and detailed approach to modelling the mentioned items. Thus, this paper focuses in detail on fragility modelling and restoration time. So that the lifetime and the correlation of distribution network components are also considered in the mentioned modelling.

On the other hand, providing correct resilience quantification metrics and using suitable resilience strategies to enhance the power system resilience will lead to systems with high resilience and low cost (HRLC) from system design perspectives. Accordingly, the present study aims to propose comprehensive metrics for resilience quantification. Hence, two comprehensive quantification metrics for the distribution power systems will be defined based on the vulnerability rate (R_v) and restoration rate (R_r).

* Corresponding author.
E-mail addresses: f.dehghani@shirazu.ac.ir (F. Dehghani), m.mohammadi@shirazu.ac.ir (M. Mohammadi), mazaher.karimi@uwasa.fi (M. Karimi).

https://doi.org/10.1016/j.ijepes.2023.109089
Received 7 August 2022; Received in revised form 21 January 2023; Accepted 9 March 2023
Available online 23 March 2023
0142-0615/

Nomenclature

A. Sets and Indices

l	Overhead distribution line index
c	Overhead distribution lines conductor index
pl	Power distribution poles index
t	Time index
P_f	Failure probability index

B. Parameters and Constants

$G(x)$	Performance function of a structural member
S_{com}	Strength of structural members
S_0	Initial strength of poles
L_{com}	Load demand caused by wind speed
x_S	Random strength parameters
x_L	Random load demand parameters
d_S	Deterministic strength parameters
d_L	Deterministic load demand parameters
$F_r(v)$	Structural fragility
v	Wind speed
m_r	Median of the fragility function
ξ_r	Logarithmic standard deviation of intensity measure
$\phi[0]$	Standard normal probability integral
P_f^{cpl}	Failure probability of a central pole in three poles system
P_f^{apl}	Failure probability of adjacent poles in three poles system
P_f^{stpl}	Failure probability of a three-pole system
$P_{f,pl}^l$	Failure probability of overhead line due to breakdown poles
$P_{f,sec}^l$	Failure probability of overhead line due to breakdown sections
$P_{f,c}^{sec}$	Failure probability of individual section due to failure of conductor
P_f^{pl}	Failure probability of pole
P_f^c	Failure probability of conductor
N_{pl}^l	Number of poles of line l
N_{dpl}^l	Number of damaged poles of line l
N_{sec}^l	Number of sections of line l
N_{dsec}^l	Number of damaged sections of line l
N_{sp}^{sec}	Number of spans of section
N_r	Number of running times of the MCS
N_f	Number of failure events in MCS
ttr_{pl}^n	Time to repair damaged poles under normal conditions
ttr_{sec}^n	Time to repair damaged sections under normal conditions due to failure of conductor
ttr_{dc}	Required time to repair damaged components
ttr_l	Time to repair overhead line
ttr_s	Time to return the system to a resilient state
t_w	Waiting time for the end of extreme event
t_a	Required time to arrive at the fault location
t_r	Operator response times to contingencies and coordination with the repair crews
t_o	Occurrence time of the extreme event
t_d	Time of disturbance occurrence
t_{vs}	Time to a disrupted state
t_e	End time of the extreme event
t_{rs}	Time to restoration state
S^l	Status of overhead distribution line l
F_c^l	Functional states of the conductor related to line l
F_{pl}^l	Functional states of the poles related to line l
$R(i)$	Change/growth rate of the system performance level
R_a	Average change rate
R_r	Restoration rate
R_v	Vulnerability rate
$P(t)$	Performance level of the system over time
P_i	Impact of the extreme event on the system performance level
α	The binary variables indicate an overhead line outage due to damaged poles (Equal 1 for damaged overhead lines due to failure of poles; otherwise, it would be 0.)
β	The binary variables indicate an overhead line outage due to damaged conductors (Equal 1 for damaged overhead lines due to failure of conductors; otherwise, it would be 0.)

1.2. Brief literature review

In order to assess the resilience of a power system, the impact of extreme events on its components and infrastructure should be investigated. It is, therefore, necessary to calculate the failure probability of components in different weather states. Hence, it can be observed that the failure probability of individual towers and lines under a range of wind loading presented in [3,4] is different from the failure probability of towers due to ice disasters presented by [5]. Five methods are generally utilized to derive failure models of vulnerable components that provide input data for resilience metrics development and assessment. These are the analytical, experimental, empirical, judgmental, and hybrid methods [6]. In [7], a framework for evaluating and improving network resilience is presented. In this regard, the fragility curves were obtained using historical and experimental data related to the poles' failure according to the intensity of the incident. However, such data may be particular to the source situation or location and contain only data on occurrences recorded during the monitoring period. The component vulnerability model for snow events was proposed by [8], which developed a detailed physical-based method to account for the fault probability of overhead lines in MV and HV grids due to contact with trees. Particularly, the vertical contact due to the decreasing line sag and the lateral contact due to falling trees is modeled in this paper. Recently, researchers have shown an increased interest in using analytical and simulation-based methods to model the fragility of components. These methods, which often combine with Monte Carlo simulation (MCS) and structural analysis, capture the impact of essential design variables such as wind speed, class, age, tower and pole height, etc. [9–12]. On the other hand, major studies related to resilience in distribution systems have focused on resilience enhancement [13–16]. Therefore, the failure probability of vulnerable components has not been investigated in these studies.

The fragility model is used to calculate the failure probability of overhead lines. In [4], transmission towers are assumed to fail independently of one another, and corridor outage occurs due to a conductor failure or a tower collapse. However, the authors in [17] use the conditional failure probability of the conductor and tower to model the transmission corridor outage. The fragility of overhead lines in the distribution system is modelled by [7] and [18] as a series system, including conductors and poles. Also, falling trees have been considered in these studies. It is assumed that the fragility of different components of overhead lines is independent. Although the equipment and infrastructure used in the transmission network differ from the distribution system, in [19], the failure probability related to the distribution system's overhead line is modelled similarly to overhead lines in the transmission network. In [20], the authors presented the failure rate of overhead distribution lines using negative binomial regression without investigating the failure rate of vulnerable components such as poles.

Similar to the fragility analysis of overhead lines, determining the weather-affected restoration time of damaged lines is crucial to increase the accuracy of the resilience assessment. In many studies, restoration time models based on the severity of hurricanes have been obtained. In this way, the authors have attempted to reflect the intensity and impact of extreme events on restoration time using weight factors [4,21,22] and distribution functions [13,20,23]. Some authors also assume that the time required to repair damaged overhead lines is fixed [5,18,24]. In [25], a broader perspective is adopted that other parameters, such as the impact of fault location and size of repair crew on time restoration, have been considered in addition to the intensity of the extreme event. Similarly, the authors mentioned that extreme events and human responses could affect restoration time [26].

One of the significant challenges in resilience assessment is the development of system modelling techniques so that the complexity and interdependencies of a power system can be modelled, and the system's performance undergoing a disruption can be simulated and assessed. Analytical and MCS are the two main techniques used in power system reliability evaluation. The analytical techniques are preferable for small-scale power system configurations due to their simplicity and lower computational burden. However, simulation techniques are more suitable for modelling complex systems and operational conditions. In order to assess the effect of weather-associated on the power systems operation, the Markov process as an analytical technique is used [27–30]. This model divides the weather conditions into two states: normal and adverse. Accordingly, failure and restoration rates for each weather condition are considered different but constant.

On the one hand, due to the stochastic behaviour and space- and time-dependent nature of the extreme weather events, and on the other hand, the size and complexity of real power systems, the simulation techniques are appropriate for studies on weather-related resilience of the power system. Following this approach, the resilience of the distribution network components has been evaluated in [7] through the fragility models of poles and conductors and MCS. The Sequential Monte Carlo simulation (SMCS) is used to assess resilience in [3–5,31,32]. Using this approach can capture the multi-temporal and multi-spatial impact of the weather front as it moves across the power system.

A considerable amount of literature has been published on introducing a metric for the quantification of resilience. There are strengths and weaknesses in every available resilience quantification metric, depending on the purpose of the study and application of interest. In [22], the resilience of power systems is assessed and quantified based on the resilience achievement worth (RAW) index. The authors in [17] provided a new index as a resilience index, considering the duration of extreme events (RICD) to evaluate the resilience of the power transmission system. This index measured the system's performance level and considered the disruption characteristics. In addition, the concept of trapezoid resilience is introduced in [21], which can be considered different phases that a power system might experience during extreme events. Then, a resilience quantification metric is proposed for each phase. Furthermore, this study presented the power system's operational and infrastructure resilience concept.

In [33], a quantitative method was investigated that quantified resilience in four phases (initial steady phase, disruptive phase, recovery phase, and a new steady phase) integrated into a resilience metric. Authors in [24] proposed a quantitative framework for the resilience assessment of microgrids in response to low-probability and high-impact events. The resilience of microgrids is quantified in different phases using the vulnerability index, degradation index, restoration efficiency index, and microgrid resilience index.

The main contributions of this paper are summarised as follows:

- First, using the limit state function, the fragility curve of vulnerable elements in power distribution systems is obtained under a range of wind loads. Given that power system infrastructures are prone to deterioration over time because of decay, corrosion, etc., an age-dependent fragility curve of vulnerable components is provided. In this way, the resilience of distribution systems with different life-spans under extreme weather events was assessed.
- The failure probability of overhead lines is modelled by considering the characteristics of power distribution systems. Accordingly, a pole's failure increases mechanical forces on adjacent poles due to the short distance between poles. Consequently, the failure of poles is considered dependent on one another. Also, the overhead lines are divided into sections consisting of several spans. The conductor's failure in one span leads to a reduced failure probability in the other spans. However, the possibility of the conductor failing in other sections remains. These characteristics are used to model the failure probability of overhead lines. Besides, the restoration time is presented by considering the factors affecting the duration of overhead line restoration.
- *Resilience* can be defined as the ability to withstand extreme events and bounce back to a pre-disturbance state. Accordingly, two resilience curve-based metrics are introduced: vulnerability rate (R_v) and restoration rate (R_r). The vulnerability rate is an indicator of the ability of the power system to withstand extreme events. Likewise, the restoration rate indicates the ability of the system to bounce back to a normal state.

The remaining part of the paper proceeds as follows. Section two begins by introducing the vulnerable components of the distribution system under extreme weather events, and then the fragility of these components is modelled. In the following, the failure probability of the overhead lines is described in detail. In addition to modelling the impact of extreme events on the failure probability of overhead lines, the effect of these events on the restoration time of damaged overhead lines is also investigated. The third section concerns the method used for assessing resilience in power systems. The fourth section presents new resilience quantification metrics, focusing on system performance during and after the extreme event. Section five provides the simulation results and analysis to validate the proposed models and assessment framework. Finally, the conclusion is given in section six.

2. Failure probability of overhead distribution lines and restoration time

The first question in this study is to determine the vulnerable components of power distribution infrastructure under extreme events. Vulnerable component types can also vary depending on the type of disruptive event (flood, earthquake, hurricane, etc.). The present study considers the assessment of distribution system resilience under extreme weather conditions. Hence, the distribution poles and conductors are considered vulnerable components during hurricanes because they are not designed to withstand high wind speeds. Next, to appropriately assess the resilience of the distribution system, the failure probability of the components mentioned above must be calculated, followed by the failure probability of the overhead distribution lines under extreme weather events. Due to a lack of data and large uncertainties involved, other failure modes, such as failure due to falling trees and flying debris that may impact poles and conductors during strong winds and contribute to their failure, are not considered in this paper. Another crucial parameter in the assessment of resilience that should be evaluated is the restoration time of the damaged equipment. In the following, the mentioned topics will be examined in more detail.

2.1. Fragility analysis

The failure probability of power system components depends on weather conditions. A fragility analysis is required in order to calculate the failure probability. For fragility analysis, the limit state or performance function of a structural member is defined as [12,34]:

$$G(X) = S_{com}(x_S, d_S) - L_{com}(x_L, d_L) \quad (1)$$

The failure probability or non-performance of the structural members is defined as ($G < 0$), which means the load demand is greater than the strength ($S_{com} < L_{com}$). The MCS is utilized to calculate the failure probabilities. As discussed above, the failure occurs if the $G(x)$ value is less than 0. As a result, failure events are identified by checking the sign of $G(x)$ for different values of random variables. Hence, the failure probability (P_f^{com}) is calculated by counting the number of times the applied load on the structure is greater than its strength.

$$P_f^{com} = \frac{N_f}{N_r} \quad (2)$$

The fragility curve demonstrates the failure probability of vulnerable components in the power distribution system for a specific load. This curve can be provided by the lognormal cumulative distribution function [11].

$$F_R(v) = \phi\left[\frac{ln(v/m_r)}{\xi_r}\right] \quad (3)$$

The fragility of the timber poles and conductors under wind loading can be evaluated using the method suggested in [10,35]. This approach can be used to calculate the failure probability of vulnerable components made with different material types, such as timber or steel poles.

The timber poles are made of organic materials, and due to fungal attacks, insects and other living organisms are susceptible to decay. Typically, the decay of timber poles occurs in areas where they come into contact with the ground. The decay rate of timber poles depends on many factors, such as timber species, climatic conditions (rainfall, humidity, and temperature), the nature of fungal and insect attacks, and soil factors. Therefore, as the age of the poles increases, their strength decreases. The strength remaining of the poles as a function of time, considering the probability of decay, is modelled by:

$$S_{pole}(t) = S_0\left[1 - min(max(a_1 t - a_2, 0), 1).min\left(max\left(b_1 t^{b_2}, 0\right), 1\right)\right] \quad (4)$$

The values of constant coefficients a_1, a_2, b_1, and b_2 were evaluated as 0.014418, 0.10683, $1.3 \times 10^{(-4)}$, and 1.846, respectively, from the regression analysis [9].

Another vulnerable component of the distribution system under extreme weather events is conductors. Overhead distribution lines consist of several spans, and they are very long. Therefore, modelling the entire distribution line is practically impossible. To resolve this problem, assumed that all spans are the same. So, the failure probability of only one span is calculated and extended to the entire distribution line. A full discussion of the fragility analysis of vulnerable components lies beyond the scope of this study. For further details, the interested reader may refer to [9]–[12,35]. Although electric utility companies have inspection and maintenance schedules to ensure that the poles' strength does not fall below a certain value, the methods used by these utilities have many uncertainties. Therefore, in this study, timber maintenance is not considered. Therefore, the fragility analysis determines the individual failure probability of two vulnerable components, namely the poles and conductors in overhead distribution lines (see Fig. 1).

2.2. Failure probability of overhead distribution lines

The collapse of poles and the breakdown of the conductor along an overhead line cause the entire line to be disconnected. Hence, the failure probability of overhead lines is calculated using the failure probability of poles and conductors as vulnerable components under extreme weather events, which will be explained as follows.

2.2.1. Failure probability of overhead line due to failure of poles

The failure probability of the overhead line is different from the failure probability of the transmission line. Failure occurs if the conductors are broken or dropped to the ground. Therefore, the failure of a single pole may not necessarily lead to the failure of the overhead line. However, the failure of a single pole due to load sharing increases the mechanical forces on adjacent poles. If the central pole fails, the adjacent poles may also fail. In this respect, the failure probability of the overhead distribution lines is calculated using the failure probability of the three consecutive poles system (interested readers can refer to [34] for more information). The failure probability of a three-pole system that is applied to each pole along the overhead distribution line can be written as follows:

$$P_f^{stpl} = P_f^{cpl}\left[2P_f^{apl} - \left(P_f^{apl}\right)^2\right] \quad (5)$$

The poles in the distribution lines are connected in series. Assuming

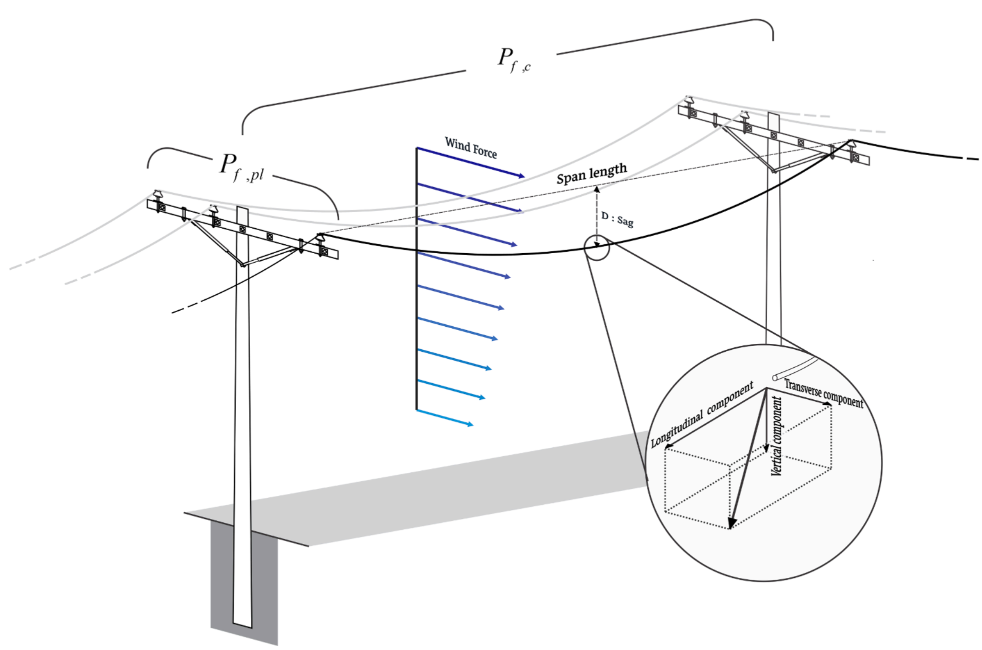

Fig. 1. Typical distribution pole for three-phase main feeder.

that the failure probability of the overhead lines is caused by the failure of poles, considering the three-pole system, all failure modes can be fully independent or fully dependent, given by (6) and (7), respectively.

$$P^{l}_{f,pl} = 1 - \left(1 - P_f^{stp}\right)^{N^{l}_{pl}} \tag{6}$$

$$P^{l}_{f,pl} = max\left[P_f^{stpl}\right] \tag{7}$$

These equations represent the upper and lower bounds of the failure probability of overhead lines due to the failure of poles. Determination of the exact failure probability requires knowledge of the correlation coefficient between poles in a line, which can vary depending on the location of each pole relative to a failed pole. In this paper, instead of the failure probability of single poles, the failure probability of three-consecutive pole systems is applied to each pole along a line. Hence, failure modes in the overhead distribution line due to the failure of poles are considered dependent. However, this dependence is limited to three poles (the central pole and two adjacent poles) because the failure of a central pole(i) can cause the failure of either of its adjacent poles ($i-1$ or $i+1$). If information about load sharing after the failure of the central pole to adjacent poles is available, this model can be expanded to a five-consecutive pole system and more. The exact failure probability of overhead lines lies somewhere between the provided bounds. However, (6) as an upper bound of failure probability is used for conservatism in this paper.

2.2.2. Failure probability of overhead line due to failure of conductors.

Besides the poles, failure of the conductors leads to the outage of the overhead lines. It is impossible to model the overall system to calculate the failure probability of overhead lines because they are very long and include many sections and spans. This problem can be solved by modelling the failure probability of a part of the overhead line and generalising it to the remainder of the lines. The sections are connected in series and contain some spans and continuous conductors. The failure probability of the overhead lines due to conductors' breakdown is obtained using the failure probability of sections. The failure of conductors in one span decreases the failure probability of conductors in other spans for each section. In addition, a failure in one or more spans of a section has the same result and will lead to an outage of the overhead lines. According to these assumptions, the failure probability of sections using the binomial distribution can be calculated as follows:

$$P^{sec}_{f,c} = \binom{N^{sec}_{sp}}{1}.P^{c}_{f}.\left(1 - P^{c}_{f}\right)^{N^{sec}_{sp}-1} = N^{sec}_{sp}.P^{c}_{f}.\left(1 - P^{c}_{f}\right)^{N^{sec}_{sp}-1} \tag{8}$$

The sections in the overhead distribution lines are connected in series. Therefore, the failure probability of an overhead line due to the failure of sections is given as follows:

$$P^{l}_{f,c} = 1 - \left(1 - P^{sec}_{f,c}\right)^{N^{l}_{sec}} \tag{9}$$

Fig. 2 presents the summary of failure probability related to different parts of the overhead distribution line. The restoration time of damaged overhead lines will be argued in the following.

2.3. Restoration time

Under extreme weather events, the overhead lines will be subjected to a new failure rate, so a new restoration time must be calculated. When the power distribution system components experience an outage, data on damaged lines are collected. Then crews are allocated to repair the damaged components, and after repairing the damaged lines, the distribution system returns to its normal state.

Following a weather event, the repair process depends on several factors, such as weather intensity, the location of the affected lines, the size of the repair crew, and the repair or replacement of a damaged component. An accurate model of restoration time should be considered to increase the accuracy of the resilience assessment of the power systems. For the safety of repair personnel and to determine the worst impact of an extreme weather event on the distribution system, it is believed that damaged components cannot be fixed during a severe event. As a result, after the extreme event is over, repair crews are dispatched to the affected lines.

Concerning the discussion above, the proposed model of restoration time is as follows:

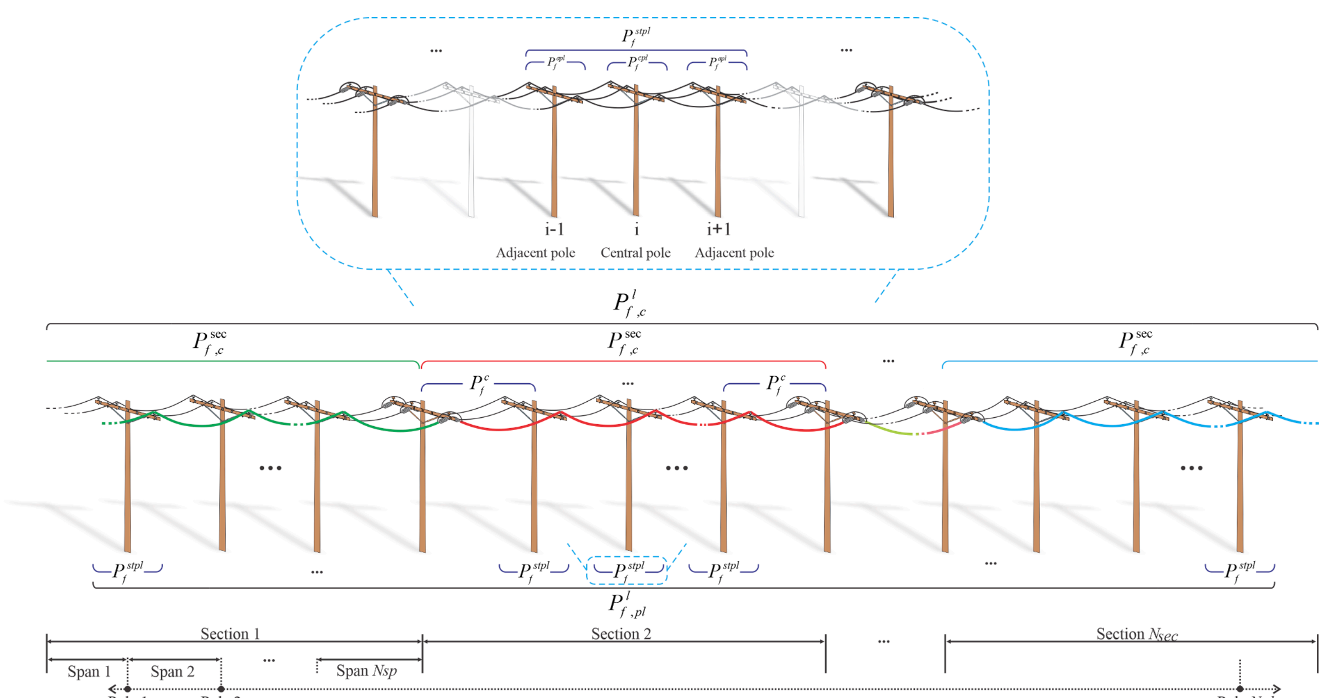

Fig. 2. Failure probabilities of different parts of the overhead distribution line.

- Waiting time

As discussed earlier, it is assumed that damaged components cannot be fixed during an extreme weather event, and these components must wait for the severe event to end. Note that the occurrence time of the extreme event may not be the same as the time of the disturbance in the power systems. Hence, the time interval between the time of disturbance occurrence and when the extreme event ends is defined as " *waiting time* " and calculated as follows:

$$t_w = t_e - t_d \tag{10}$$

- Arrival time

According to the distance between the fault location and the repair crew's departure location and considering the average speed of vehicles, the time it takes for the repair crew to arrive at the fault location must be considered. Hence, the time it takes for the repair crew to arrive at the fault location is defined as " *arrival time* " and calculated as follows:

$$t_a = \frac{D}{V_s} \tag{11}$$

Due to the lack of data on the repair crew's departure location in this study, the required time to arrive at the fault location is modelled as a probability distribution using the Poisson random variable.

- Repair time

In order to estimate the time to repair damaged overhead lines, broken components must be identified and counted. The number of potentially damaged components in each line is obtained using the failure probability of overhead lines due to poles or conductors and their total number in overhead lines.

$$N^l_{dpl} = N^l_{pl} \times P^l_{f,pl} \tag{12}$$

$$N^l_{dsec} = N^l_{sec} \times P^l_{f,sec} \tag{13}$$

By multiplying the number of damaged components by the required time to repair one of them under normal conditions, the required time to repair damaged components is calculated as follows:

$$ttr_{dc} = N^l_{dpl} ttr_{pl} \alpha + N^l_{dsec} ttr_{sec} \beta \tag{14}$$

- Response time

Lack of individual situation awareness leads to the incorrect actions of system operators and inadequate response times to contingencies. Furthermore, the ineffective coordination of the crew repairers and system operators leads to delays in restoring damaged overhead lines. So, the human response delay in restoration must be considered.

Taking into account the mentioned topics time to restore the damaged overhead line (ttr_l) can be calculated as follows:

$$ttr_l = t_w + t_a + ttr_{dc} + t_r \tag{15}$$

The overall timeline of power system resilience and the status of an overhead line are illustrated in Fig. 3. In the period from t_d to t_{vs}, the vulnerable overhead lines that are subjected to extreme weather events go out of service. Then, between t_r and ttr_s, after the repairs are completed, these lines are returned to an operational state that increases the system's performance and, as a result, its resilience. It is worth noting that overhead lines can be classified as operational or damaged during extreme events. Once an overhead line outage occurs, all customers downstream will lose power, and the overhead line is in a damaged state. After the extreme event is over, repair crews are dispatched to the affected lines. Then, by repairing the damaged components, the damaged overhead lines will return to their operational state. The following will further discuss the power system performance under extreme events and resilience curves.

3. Resiliency assessment framework

Extreme weather events such as hurricanes move across a power distribution system. The modelling of the weather impact on the operation of a large-scale power system would require a simulation approach to capture the stochastic behaviour of the weather, both space- and time-wise. Hence, SMCS is utilized to evaluate the weather's effect on the power distribution system. Under extreme weather events, the distribution system's performance level should be evaluated to determine resilience by considering supply, infrastructure, and demand changes. This paper focuses on changing infrastructure policies, such as the status of overhead lines determined by the functional states. The input of the functional states is the failure probability of overhead lines due to vulnerable components, and the output of that is overhead line status. Overhead lines can be considered in two states: operational and damaged. Hence, the outputs of the functional states are 0 and 1, which signify the damaged and operational states.

The related vulnerable component failure probability of the overhead lines in every step of the SMCS procedure is continuously updated according to the prevailing weather conditions. This update provides a realistic model of the weather event as a continuously fluctuating phenomenon. The failure probability of overhead lines will also be updated by updating the weather conditions. After that, the failure probability is compared with a uniformly distributed random number ($r\ U(0,1)$) to determine the overhead line functional states in the form of:

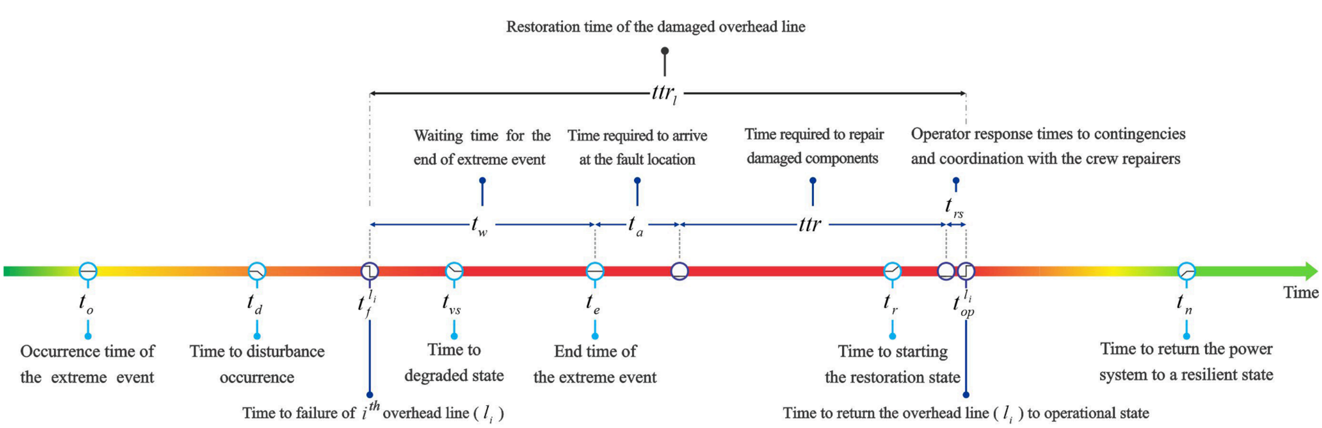

Fig. 3. The overall timeline of a power system's resilience and the status of an overhead line under extreme events.

$$F_c^l\left(P_{f,sec}^l, r\right) = \begin{cases} 1 & if \quad P_{f,sec}^l < r \\ 0 & if \quad P_{f,sec}^l > r \end{cases} \tag{16}$$

$$F_{pl}^l\left(P_{f,pl}^l, r\right) = \begin{cases} 1 & if \quad P_{f,pl}^l < r \\ 0 & if \quad P_{f,pl}^l > r \end{cases} \tag{17}$$

Finally, the status overhead lines can be obtained as:

$$S^l = F_c^l \times F_{pl}^l \tag{18}$$

While the functional states of the pole and conductor or both equal zero, the overhead line is in the damaged state ($S^l = 0$). Thus, the overhead line is in the operational state when the results of both functional states equal one ($S^l = 1$). The overhead line's status can be determined using the probabilistic framework provided for each simulation step. Following determining the state of overhead lines, the time to restoration for damaged ones should be generated as described previously.

It should be noted that most distribution systems are radial systems. In such systems, there is a unique path from the power source to each customer. Hence, if there is a fault at any point in an overhead line, all customers downstream of the point will lose power. When multiple overhead lines are outage, the power distribution system is divided into several subsystems. There are two possible situations for each subsystem in this condition: (i) it does not have distributed generation resources, and (ii) it has one or more distributed generation resources. In the first situation, a lack of distributed generation resources leads to a loss of load at buses. The second situation is divided into two parts. The distributed generating resources in the subsystem supply the customer's demands in the first portion. In the second part, these resources cannot supply all consumer demands, resulting in load shedding until supply and demand are balanced. Afterwards, the load-flow analysis is performed using the backward/forward sweep method in every simulation step to model the distribution system's behaviour under real-time operating conditions. These steps are repeated, and the results are stored until the end of the simulation. Finally, the distribution system's resilience can be assessed using the recorded data of the distribution system's performance level

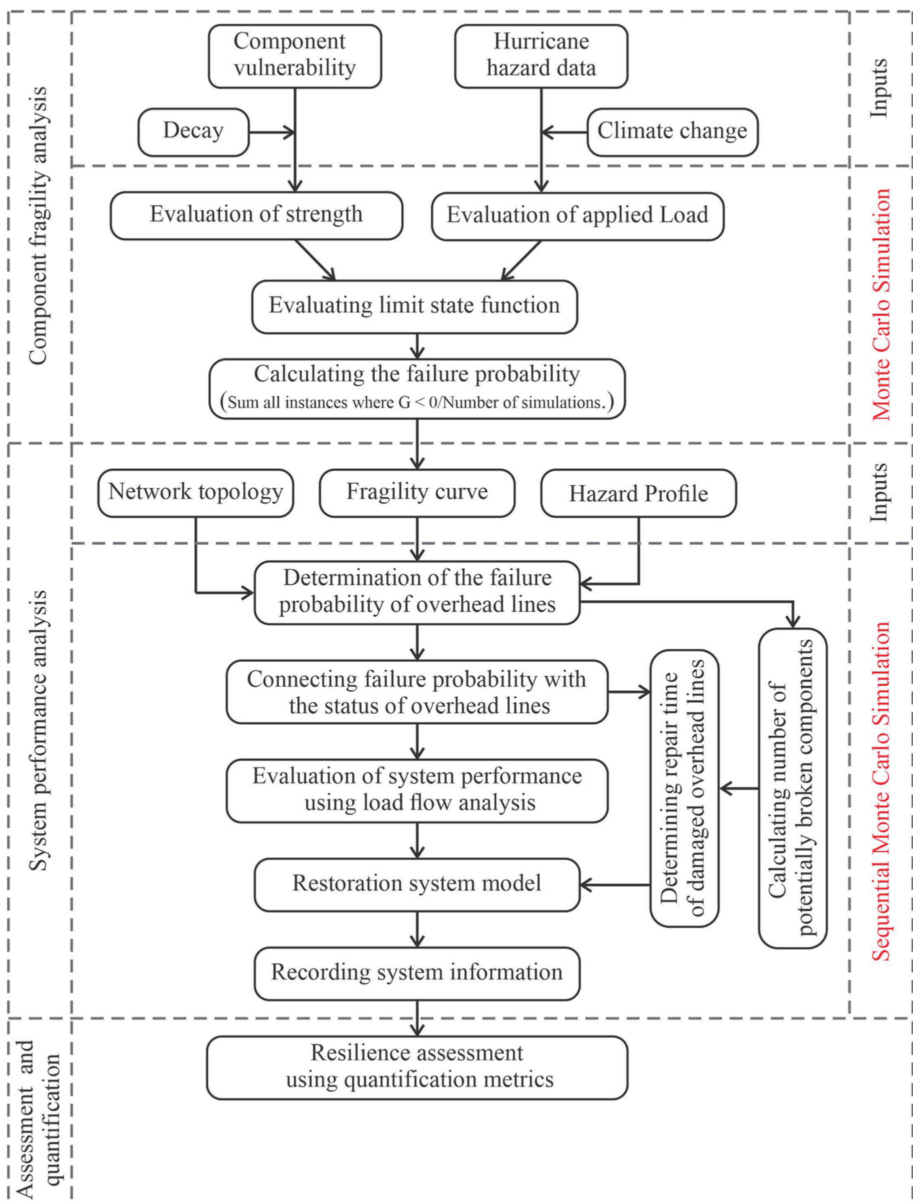

Fig. 4. A general flow chart of resilience assessment in power systems.

before, during, and after extreme weather events.

In summary, the main execution steps for resilience assessment of the power system can be illustrated as a flowchart in Fig. 4. In general, resilience assessment can be divided into three sections. In the first section, the failure probability of vulnerable components as a function of the extreme weather parameter is calculated, and then the failure probability of overhead lines is modelled. The following section evaluates the system's performance under extreme weather events. Different performance measures, such as the percentage of total or critical loads, number of supplied customers, number of survived components, etc., can represent power system performance. In this paper, the system performance is assessed by the supplied load. In the third section, the power system's resilience is assessed and quantified using the recorded information about system performance under extreme weather events.

4. Resilience quantification metrics

According to the resilience definition, a resilient system has two main features. The first feature of an engineered system is its ability to withstand or survive disruptive events, and the second one is its ability to bounce back to a pre-disrupted state. Hence, the vulnerability and restoration rates are proposed as resilience indicators in this respect, which will be discussed in the following.

The resilience of engineering systems is typically represented and assessed using a resilience curve with the horizontal axis of time and the vertical axis of distribution system performance. This curve is created with the same time resolution as the weather model. The time resolution of the weather model depends on weather data availability. Although higher time resolution leads to accuracy in the assessment, the hourly time resolution is considered in this study (t^*). The change rate can be obtained in systems that have changes in performance levels. The change rate of the system performance level at each interval time between t_i and $t_i - t^*$ can be calculated as follows. In this regard, we subtract one unit from the value of the growth rate. If the growth rate is positive, it indicates an increase in system performance; if it is negative, it means the system's performance is declining.

$$R(i) = \frac{P(t_i)}{P(t_i - t^*)} - 1 \tag{19}$$

The above relation calculates the system's performance level change rates over a specific time duration. At this time, the average of these values should be obtained. There are three means to calculate the average of numbers in the data set: harmonic mean, arithmetic mean, and geometric mean. Usually, the geometric mean is used to calculate the average change rate of a variable over a particular time period. Also, unlike the arithmetic mean, the skewed data effect on the geometric mean is very small [36]. Hence, the average change rate of the system performance level is achieved using the following geometric mean. In this case, the growth rate is increased by the same unit that was previously deducted from it.

$$R_a = \sqrt[N_{ti}]{(R(1)+1) \times \cdots \times (R(N_{ti})+1)} - 1 = \sqrt[N_{ti}]{\prod_{i=1}^{N_{ti}} (R(i)+1)} - 1 \tag{20}$$

Rewriting (20) by (19), the average change rate is described as:

$$R_a = \sqrt[N_{ti}]{\left(\frac{P(t_1)}{P(t_1 - t^*)}\right) \times \left(\frac{P(t_2)}{P(t_2 - t^*)}\right) \times \ldots \times \left(\frac{P(t_{N_{ti}})}{P(t_{N_{ti}} - t^*)}\right)} - 1 \tag{21}$$

If $t^* = 1h \rightarrow t_i = t_{i+1} - t^*$, average change rate calculated as follows:

$$R_a = \sqrt[N_{ti}]{\frac{P(t_{N_{ti}})}{P(t_1 - t^*)}} - 1 \tag{22}$$

The resilience curve can be used to calculate the average change rate of the power distribution system's performance level during extreme weather events. Fig. 5 shows an overview of the change in the performance of a typical power system under extreme events over time. Generally, there are three phases in the distribution system resilience concept; these states are described as the unreliability state, the degraded state, and the restoration state. In the unreliable state, the system performance level decreases. Then, the system is in a degraded state until the restoration process begins. The system's performance level increases in the restoration state until it operates normally. The performance of newly established power distribution systems may not change during the first hours of the occurrence of extreme events due to the withstand of their infrastructure. However, as the lifespan of these systems increases, their withstand duration under extreme events decreases. The process of reducing system performance stops at the end of extreme events. However, this process may be stopped when the power system is under extreme weather conditions. According to the concept of resilience and the discussions mentioned above, two new indexes have been proposed to assess the power system's resilience:

$$R_v = \sqrt[t_e - t_o]{\frac{P(t_e)}{P(t_o)}} - 1 \tag{23}$$

$$R_r = \sqrt[ttr_s - t_e]{\frac{P(ttr_s)}{P(t_e)}} - 1 \tag{24}$$

The vulnerability rate (R_v) means how much the system performance level changes under extreme weather events per hour and is related to the unreliability state. Likewise, the restoration rate (R_r) indicates the average system performance increase after the extreme event's end per hour. This index is also related to the degraded state and restoration state. Therefore, according to the concept of resilience, the two main features of withstanding and quick recovery can be quantified using these indicators. Besides, these indexes can be used to compare two separate systems under one type of extreme event regardless of their duration.

The impact of the extreme event on system performance is equal to the difference between the initial and final performance levels in the unreliability state, which is calculated as follows:

$$P_i = P(t_o) - P(t_e) = 1 - (1 + R_v)^{t_e - t_o} \tag{25}$$

As a result, the maximum quantity of system performance level degradation is predictable by forecasting the duration of future extreme weather events and considering the vulnerability rate of the distribution system based on past extreme events. Also, depending on the vulnerability and restoration rate, the time required to return the system to a resilient state is given by:

$$ttr_s = \frac{log\left(\frac{1}{(1+R_v)^{t_e - t_o}}\right)}{log(1 + R_r)} \tag{26}$$

Proposed resilience indicators can support decision-making concerning system management and plans such as expansion planning and resource allocation to enhance systems. In this context, strengthening infrastructure assets through hardening measures must be considered to reduce the vulnerability rate of the power system against disruptive events. On the other hand, optimal equipment placement, network reconfiguration, and utilization of smart grid technologies can improve the restoration rate. It should be noted here that power systems' vulnerability and restoration rates under different extreme weather events can be compared. Therefore, the power system performance under different extreme weather events that a power system may be exposed to during its lifetime will be compared using the proposed indicators. It is also possible to examine the impact of resilience enhancement measures, such as reinforcing strategies, optimal equipment placement, etc., on power systems by the proposed indicators. Also, using the restoration and vulnerability rates of power systems, their behaviour can be predicted in the face of future extreme weather

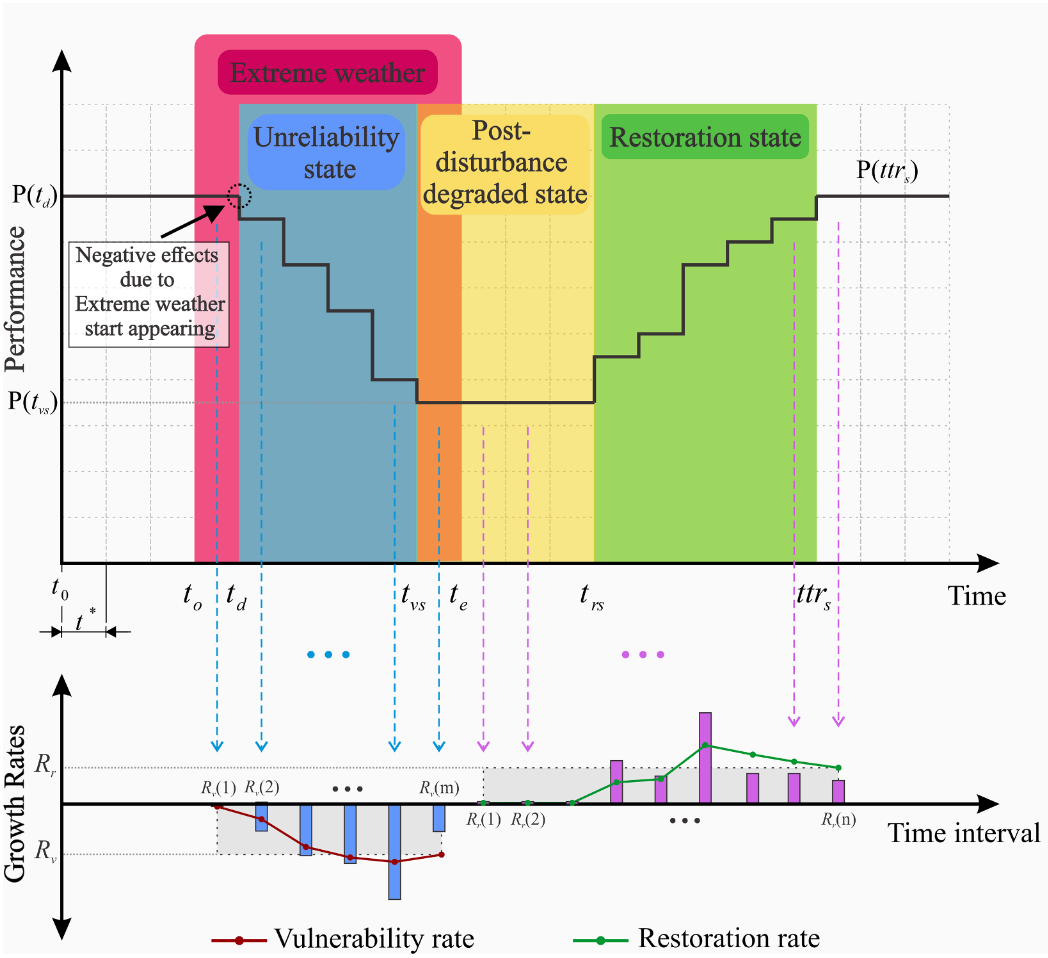

Fig. 5. The novel concept of notional engineering resilience behaviour following a disruptive event.

events. Accordingly, by predicting the duration of future extreme weather events and knowing the vulnerability and restoration rate, it can be determined how much the system performance level may decrease and how long it takes to return to its normal state.

5. Test network and simulation

The resilience assessment process is performed using a case study on the IEEE 69-bus test radial distribution system. Total system loads are 3802.19 kW and 2694.06 kVAr labelled from 1 to 69. This test system contains 69 buses, 68 distribution corridors, and 68 sectionalizing switches. The initial states of all the sectionalizing switches are closed. Also, this test system has seven lateral lines. The parameters and load data are given in [37]. Ideally, to accurately assess the resilience of the distribution systems, the number of poles, span lengths, and geographical data such as the location of the poles should be included in distribution system modelling. Due to the lack of data, we have assumed that the number of sections in each distribution corridor exposed to the hurricane is random ($N_i^{span} \sim$ U (3,20)). It is also assumed that any section includes ten spans, and the span length for all spans is the same and equals 45 m.

First, the fragility analysis of the conductor and poles, taking into account their lifespan by the limit state function at various wind speeds, is calculated. Accordingly, the MCS method was used. In this method, one million random numbers for the variables involved in the formulation for different wind speeds were generated and then this function was assessed. Failure occurs when the structure's strength is insufficient to withstand the applied load ($G(x) < 0$).

Note that the failure probability at a specific wind speed equals the ratio of failures to the total number of simulations. Following this approach, the fragility curve of the conductor and timber poles, taking into account their lifespan, was obtained. Most electric utilities use 30 to 40 years as the estimated service life of timber poles [38]. Therefore, to assess the age-dependent resilience of power distribution systems, 40-year-old timber poles were considered. Also, given that the aim here is the age-dependent resilience assessment of the distribution systems, another period over which minimum system performance is assessed is taken as 60 years old to allow comparison. As shown in Fig. 6a., the decay of timber poles causes them to become more vulnerable. Hence, their failure probability at lower wind speeds increases. The results obtained from the analysis of fragility poles and conductors' parameters are summarized in Table.1.

As explained earlier, the restoration time of the overhead distribution lines depends on several factors, such as weather intensity, location of the affected area, etc. When a vulnerable component's fault or collapse occurs, the restoration time of the damaged line is generated randomly. The uncertain parameters in the calculation of the restoration time are summarised in Table 2.

Millions of consumers in Florida experienced power outages due to the Irma hurricane in September 2017 [39]. In this study, to create a time-series wind profile, the historical weather observations of this hurricane for one week related to areas of Orlando were obtained from [40]. This wind profile is used as input in the simulation, as shown in Fig. 7. Note that in weather-related studies, weather conditions are considered homogeneous within the entire region of the distribution system. Hence, the distribution system is exposed to the same weather

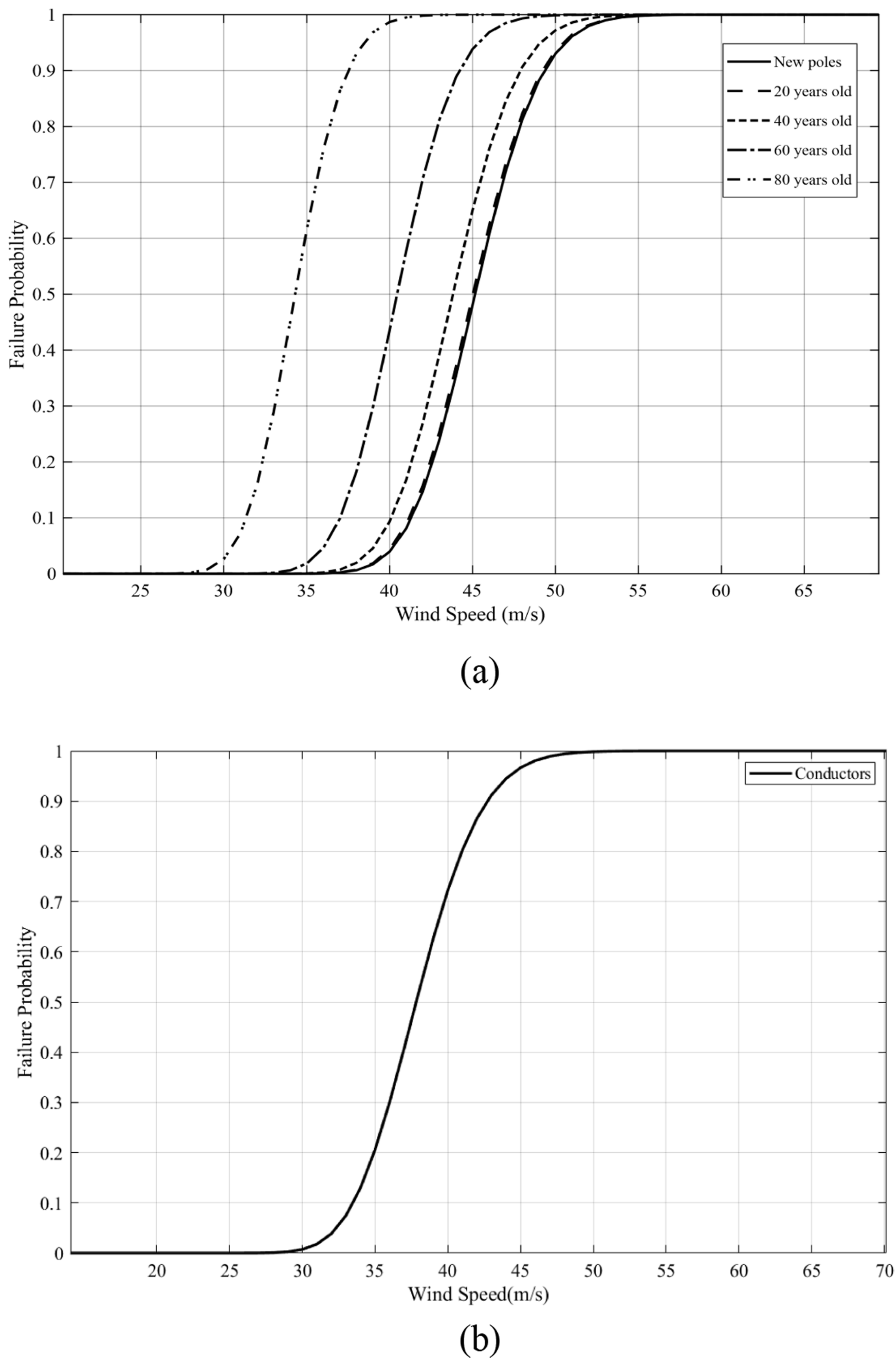

Fig. 6. Fragility curves of (a) timber poles at 0, 20, 40, 60, and 80 years (b) conductors.

Table 1
Lognormal parameters for fragility curve of the poles and conductors.

Age	$ln(m_r)$	ξ_r
Timber pole		
New poles	3.81	0.135
20-year-old	3.80	0.134
40-year-old	3.78	0.136
60-year-old	3.70	0.135
80-year-old	3.53	0.137
Conductors		
0 to 20 years old	3.63	0.0946

Table 2
Restoration time parameters of overhead distribution lines based the timber poles and conductors.

'Parameter	Distribution function	Vulnerable components	
		Conductor	Timber pole
ttr	Normal	$\mu = 4h, \sigma = 1h$	$\mu = 5h, \sigma = 2.5h$
t_a	Poisson	$\lambda = 3h$	$\lambda = 3h$
t_r	Normal	$\mu = 15min, \sigma = 5min$	$\mu = 15min, \sigma = 5min$
t_w	—	*	*

* Depending on the time of damage occurrence.

conditions everywhere. Furthermore, the SMCS captures the extreme weather event's space-and time-dependent nature.

The distribution system's resilience could be affected by various features. This study assessed the distribution system's resilience by considering different ages under the same weather conditions. The resilience curve was obtained based on the distribution system's performance, or, in other words, the amount of power required by consumers. As indicated in Fig. 8, the performance of distribution systems 40 and 60 years old was reduced at the start of the hurricane. In contrast, the new distribution system has withstood the storm for several hours. As a result, it can be argued that timber poles become more vulnerable as their lifespan increases. Hence, they are more susceptible to failure during extreme weather events, reducing the resilience of distribution systems.

Although the new distribution system is subjected to extreme weather events, its declining performance has stopped. However, this process continues in distribution networks that are 40 and 60 years old until the end of the extreme weather event. From Table.3, we can see that the vulnerability rate for the new power distribution system ($R_v = -2.396$) is lower than for the 40-year-old distribution system ($R_v = -4.144$). It can be observed that the 60-year-old power distribution system has the most reduction in performance level compared to other distribution networks with a shorter lifespan. Also, the vulnerability rate for the 40-year-old distribution system is lower than for the 60-year-old distribution system ($R_v = -6.413$).

Depending on the emergency plans and intensity of extreme weather events, the time it takes for the power systems to return to a normal state will be different. In other words, a distribution system that is 40 or 60 years old can be planned so that, relative to the new distribution system, it returns to a normal state faster. Assuming that the planning for the restoration of the distribution system at different ages is the same, it can be observed that the growth rate of restoration of new distribution systems is higher than that of distribution systems aged 40 and 60 years old. After the extreme weather event, the power distribution system is in a degraded state. In contrast to the 40- and 60-year-old distribution systems, the infrastructure of the new distribution system is less affected. Hence, the vulnerable points have been identified earlier, and adequate repair crews will be sent to repair them. Therefore, the new distribution system remains in a degraded state for a shorter period of time.

The results of this study indicate a significant correlation between the age of power distribution systems and the resilience of the systems. This feature is demonstrated through the proposed indicators for assessing resilience. With the ageing distribution network, the vulnerability rate increases and the restoration rate decreases. Also, according to the obtained data, with the age of power distribution systems, the impact of extreme weather events on the performance of this system will increase. To assess resilience, the ratio of area under the curve $P(t)$ to the total area between t_n and t_o has been calculated that indicates energy supplied. The area under the resilience curve depends on the vulnerability rate, the restoration rate, and the duration of the extreme event. As a result, decreasing the vulnerability rate or increasing the restoration rate increases the area under the resilience curve to the total area ratio. Following this approach, the ratio of area under the curve $P(t)$ to the total area is expected to reduce with the increasing age of distribution systems.

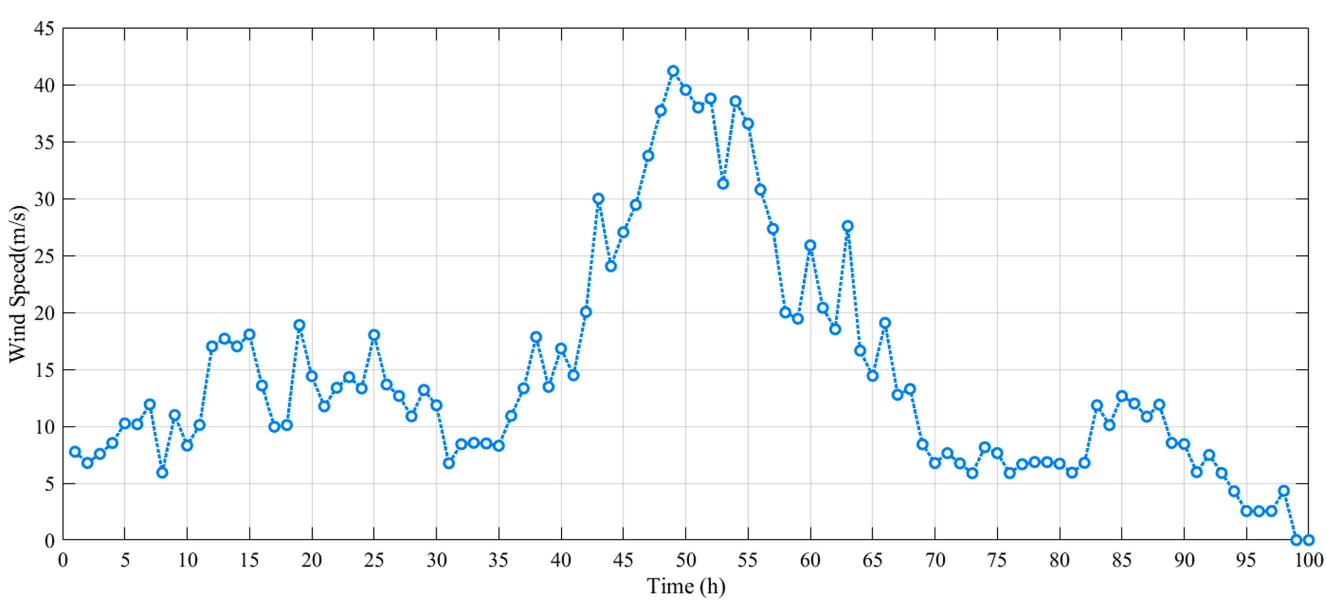

Fig. 7. The hourly wind profiles.

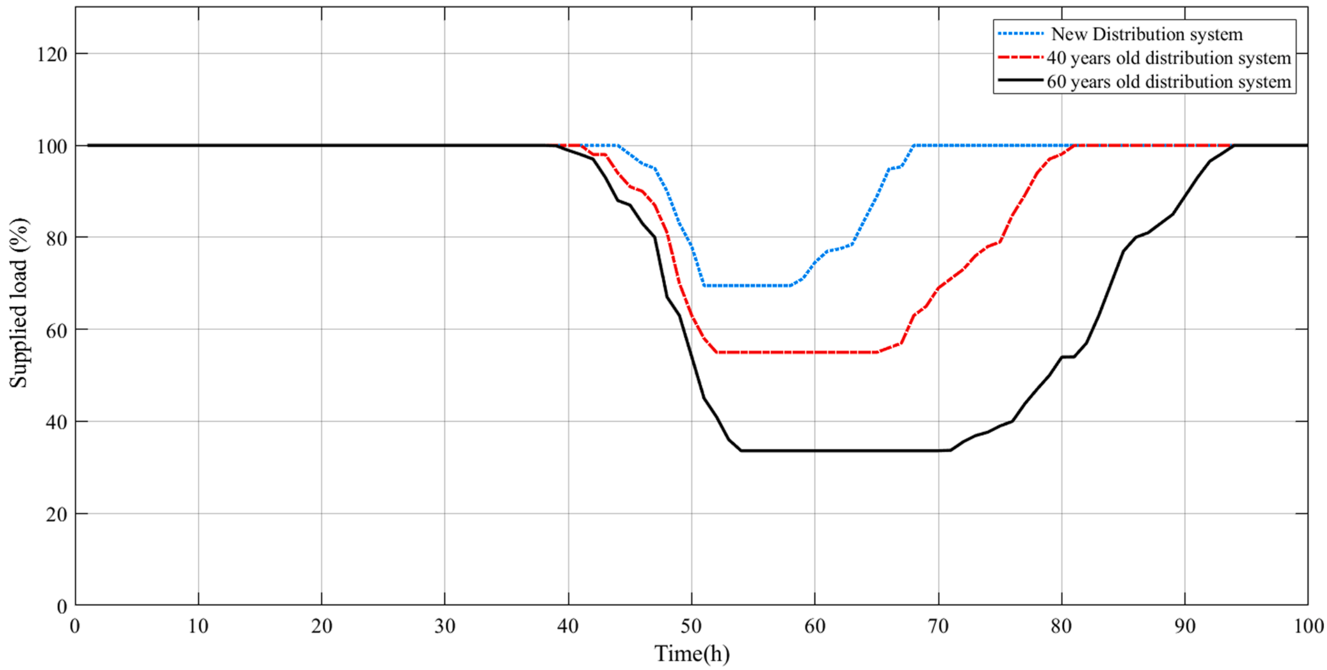

Fig. 8. Resilience curve of distribution system at 0, 40 and 60 years.

Table 3
Resilience indicators for different ages of the distribution system.

Resilience indexes	Description	New	At 40 years	At 60 years
$R_v[\%/h]$	Vulnerability rate	−2.396	−4.144	−6.413
$R_r[\%/h]$	Restoration rate	3.07	2.37	2.04
$P_i[\%]$	Extreme event impact on system performance	30.50	47.00	63.40
$ES[\%]$	The ratio of area under the curve P(t) to the total area between ttr_s and t_o	92.07	80.17	59.60

6. Conclusion

This paper provides a probabilistic and detailed methodology to assess the resilience of power distribution systems subjected to hurricanes. In this regard, the fragility curve of the pole and conductor was calculated, and then the failure probability of the poles, having regard to their dependence on one another, was modelled. Since the power system infrastructure is prone to failure over time due to decay, corrosion, etc., an age-dependent fragility analysis of poles was considered. Likewise, the resilience assessment of the system has been presented according to the different lifetimes. Due to the continuous nature of the conductors, failing a conductor in a single span reduced its failure probability in other spans. Hence, the failure probability of the overhead lines caused by failing conductors has been formulated, taking this feature into account. The restoration time of overhead lines was also modelled as a function of the possible number of damaged components and experimental parameters. The second significant finding of this paper was to provide a novel resilience quantification framework. Consequently, vulnerability and restoration rates were proposed as indicators for assessing resilience.

The numerical results indicated a significant correlation between the age of power distribution systems and the system's resilience. According to the obtained data, with the age of power distribution systems, the impact of extreme weather events on the performance of these systems will increase. So, with the ageing distribution network, the vulnerability rate increases and the restoration rate decreases. Besides, the proposed metrics, the vulnerability and restoration rate, can be used to compare several independent power systems. Also, using these metrics, the behaviour of power systems can be predicted in the face of future extreme weather events. Most studies on power distribution system resilience have been focused on resilience enhancement. Depending on the age of distribution systems, the proposed solutions to enhance resilience can differ. Therefore, it is suggested that the resilience enhancement of power distribution systems by considering the age of these systems be investigated in future studies.

CRediT authorship contribution statement

Farshid Dehghani: Conceptualization, Methodology, Software, Formal analysis, Investigation, Data curation, Writing – original draft, Visualization. **Mohammad Mohammadi:** Validation, Resources, Writing – review & editing, Supervision, Project administration. **Mazaher Karimi:** Validation, Resources, Writing – review & editing.

Declaration of Competing Interest

The authors declare that they have no known competing financial interests or personal relationships that could have appeared to influence the work reported in this paper.

Data availability

No data was used for the research described in the article.

References

[1] Matisziw TC, Murray AT, Grubesic TH. Strategic network restoration. Networks Spat Econ 2010;10(3):345–61. https://doi.org/10.1007/s11067-009-9123-x.
[2] Shi F, Qingxin and Liu, Wenxia and Zeng, Bo and Hui, Hongxun and Li. Enhancing distribution system resilience against extreme weather events: concept review, algorithm summary, and future vision. Int J Electr Power Energy Syst 138 (2022) 107860.
[3] Panteli M, Mancarella P. Modeling and evaluating the resilience of critical electrical power infrastructure to extreme weather events. IEEE Syst J 2017;11(3): 1733–42. https://doi.org/10.1109/JSYST.2015.2389272.
[4] Panteli M, Pickering C, Wilkinson S, Dawson R, Mancarella P. Power system resilience to extreme weather: fragility modeling, probabilistic impact assessment,

and adaptation measures. IEEE Trans Power Syst 2017;32(5):3747–57. https://doi.org/10.1109/TPWRS.2016.2641463.
[5] Lu J, Guo J, Jian Z, Yang Y, Tang W. Resilience assessment and its enhancement in tackling adverse impact of ice disasters for power transmission systems. Energies 2018;11(9):2272. https://doi.org/10.3390/en11092272.
[6] Dunn S, Wilkinson S, Alderson D, Fowler H, Galasso C. Fragility curves for assessing the resilience of electricity networks constructed from an extensive fault database. Nat Hazards Rev 19(1) (2018). doi: 10.1061/(asce)nh.1527-6996.0000267.
[7] Najafi Tari A, Sepasian MS, Tourandaz Kenari M. Resilience assessment and improvement of distribution networks against extreme weather events. Int J Electr Power Energy Syst 2021;125:106414. https://doi.org/10.1016/j.ijepes.2020.106414.
[8] Ciapessoni E, Cirio D, Pitto A, Pirovano G, Sforna M. Modelling the vulnerability of overhead lines against tree contacts for resilience assessment. In: 2020 Int. Conf. Probabilistic Methods Appl. to Power Syst; 2020. p. 1–6. https://doi.org/10.1109/PMAPS47429.2020.9183607.
[9] Shafieezadeh A, Onyewuchi UP, Begovic MM, Desroches R. Age-dependent fragility models of utility wood poles in power distribution networks against extreme wind hazards. IEEE Trans Power Deliv 2014;29(1):131–9. https://doi.org/10.1109/TPWRD.2013.2281265.
[10] Dagher HJ. Reliability-based design of utility pole structures. Am Soc Civ Eng Reston VA 29 (2006). doi: 10.1061/9780784408452.
[11] Bjarnadottir S, Li Y, Stewart MG. Hurricane risk assessment of power distribution poles considering impacts of a changing climate. J Infrastruct Syst 2013;19(1):12–24. https://doi.org/10.1061/(asce)is.1943-555x.0000108.
[12] Salman AM, Li Y, Bastidas-Arteaga E. Maintenance optimization for power distribution systems subjected to hurricane hazard, timber decay and climate change. Reliab Eng Syst Saf 2017;168:136–49. https://doi.org/10.1016/j.ress.2017.03.002.
[13] Ma S, Su L, Wang Z, Qiu F, Guo G. Resilience enhancement of distribution grids against extreme weather events. IEEE Trans Power Syst 2018;33(5):4842–53. https://doi.org/10.1109/TPWRS.2018.2822295.
[14] Kim J, Dvorkin Y. Enhancing distribution system resilience with mobile energy storage and microgrids. IEEE Trans Smart Grid 2018;10(5):4996–5006. https://doi.org/10.1109/TSG.2018.2872521.
[15] Wang X, Shahidehpour M, Jiang C, Li Z. Resilience enhancement strategies for power distribution network coupled with urban transportation system. IEEE Trans Smart Grid 2019;10(4):4068–79. https://doi.org/10.1109/TSG.2018.2848970.
[16] Zunnurain I, Sang Y, Mandal P, Velez-Reyes M, Espiritu J. Improving the resilience of large-scale power systems using distributed static series compensators. Int J Electr Power Energy Syst 2023;145. https://doi.org/10.1016/j.ijepes.2022.108702.
[17] Yang Y, Tang W, Liu Y, Xin Y, Wu Q. Quantitative resilience assessment for power transmission systems under typhoon weather. IEEE Access 2018;6:40747–56. https://doi.org/10.1109/ACCESS.2018.2858860.
[18] Ma S, Chen B, Wang Z. Resilience enhancement strategy for distribution systems under extreme weather events. IEEE Trans Smart Grid 2016;9(2):1442–51. https://doi.org/10.1109/TSG.2016.2591885.
[19] Luo D, et al. Evaluation method of distribution network resilience focusing on critical loads. IEEE Access 2018;6:61633–9. https://doi.org/10.1109/ACCESS.2018.2872941.
[20] Bessani M, et al. Probabilistic assessment of power distribution systems resilience under extreme weather. IEEE Syst J 2019;13(2):1747–56. https://doi.org/10.1109/JSYST.2018.2853554.
[21] Panteli M, Mancarella P, Trakas DN, Kyriakides E, Hatziargyriou ND. Metrics and quantification of operational and infrastructure resilience in power systems. IEEE Trans Power Syst 2017;32(6):4732–42. https://doi.org/10.1109/TPWRS.2017.2664141.
[22] Panteli M, Trakas DN, Mancarella P, Hatziargyriou ND. Power systems resilience assessment: Hardening and smart operational enhancement strategies. Proc IEEE 2017;105(7):1202–13. https://doi.org/10.1109/JPROC.2017.2691357.
[23] Ma S, Li S, Wang Z, Qiu F. Resilience-oriented design of distribution systems. IEEE Trans Power Syst 2019;34(4):2880–91. https://doi.org/10.1109/TPWRS.2019.2894103.
[24] Amirioun MH, Aminifar F, Lesani H, Shahidehpour M. Metrics and quantitative framework for assessing microgrid resilience against windstorms. Int J Electr Power Energy Syst 2019;104:716–23. https://doi.org/10.1016/j.ijepes.2018.07.025.
[25] Ouyang M, Dueñas-Osorio L. Multi-dimensional hurricane resilience assessment of electric power systems. Struct Saf 2014;48:15–24. https://doi.org/10.1016/j.strusafe.2014.01.001.
[26] Panteli M, Crossley PA, Kirschen DS, Sobajic DJ. Assessing the impact of insufficient situation awareness on power system operation. IEEE Trans Power Syst 2013;28(3):2967–77. https://doi.org/10.1109/TPWRS.2013.2240705.
[27] Billinton R, Singh GD. Reliability assessment of transmission and distribution systems considering repair in adverse weather conditions. Can Conf Electr Comput Eng 2002;1:88–93. https://doi.org/10.1109/ccece.2002.1015180.
[28] Liu Y, Singh C. Reliability evaluation of composite power systems using markov cut-set method. IEEE Trans Power Syst 2010;25(2):777–85. https://doi.org/10.1109/TPWRS.2009.2033802.
[29] Billinton R, Wu C, Singh G. Extreme adverse weather modeling in transmission and distribution system reliability evaluation. 14th Power Syst Comput Conf 2002; June:24–8.
[30] Billinton R, Acharya J. Consideration of multi-state weather models in reliability evaluation of transmission and distribution systems. Can Conf Electr Comput Eng 2005;2005:619–22. https://doi.org/10.1109/CCECE.2005.1557007.
[31] Zhang H, Yuan H, Li G, Lin Y. Quantitative resilience assessment under a tri-stage framework for power systems. Energies 2018;11(6), doi: 10.3390/en11061427.
[32] Fanucchi RZ, et al. Stochastic indexes for power distribution systems resilience analysis. IET Gener Transm Distrib 2019;13(12):2507–16. https://doi.org/10.1049/iet-gtd.2018.6667.
[33] Nan C, Sansavini G. A quantitative method for assessing resilience of interdependent infrastructures. Reliab Eng Syst Saf 2017;157:35–53. https://doi.org/10.1016/j.ress.2016.08.013.
[34] Taras A, Ratel G, Chouinard L. A life-cycle cost approach to the maintenance of overhead line supports. Reliab Optim Struct Syst 2020:241–9. https://doi.org/10.1201/9781003078876-30.
[35] TC on E. T. L. S. Loading. Guidelines for Electrical Transmission Line Structural Loading. Am Soc Civ Eng Reston VA 2020;241—249. doi: 10.1061/9780784415566.
[36] Lovric M. International Encyclopedia of Statistical Science; 2011.
[37] Savier JS, Das D. Impact of network reconfiguration on loss allocation of radial distribution systems. IEEE Trans Power Deliv 2007;22(4):2473–80. https://doi.org/10.1109/TPWRD.2007.905370.
[38] Mankowski M, Hansen E, Morrell J. Wood pole purchasing, inspection, and maintenance: a survey of utility practices. For Prod J 2002;52(11):43–50.
[39] Blake ES. National Hurricane Center Tropical Cyclone Report. Hurricane Lowell', no. October; 2015. p. 1–32.
[40] 'Weather Underground'; 2013. http://www.wunderground.com.